CARBON MONOXIDE EMISSION FROM SMALL GALAXIES

Harley A. Thronson, Jr.
Wyoming Infrared Observatory

John Bally
AT&T Bell Laboratories

ABSTRACT. We have searched for J = 1 → 0 CO emission from 22 galaxies, detecting half, as part of a survey to study star formation in small- to medium-size galaxies. Although we find substantial variation in the star formation efficiencies of the sample galaxies, there is no apparent systematic trend with galaxy size.

1. INTRODUCTION AND BACKGROUND

A correlation between far-infrared and CO emission from galaxies was discovered by Telesco and Harper (1980) and discussed recently and more fully by Rickard and Harvey (1984) and Young *et al.* (1986). Dust reprocesses starlight into far-infrared radiation. Massive young stars, which are signposts of ongoing star formation are usually surrounded by warm (30 to 60 K) dust which re-emits much of the radiation into the 60 and 100 μm bands surveyed by the IRAS satellite. Thus, the far-infrared flux should be a tracer of the global rate of star formation in a galaxy. To first order, the CO emission is a tracer of the principle reservoir of mass from which the stars are produced. Given that the far-infrared emission arises from dust heated by young stars, L_{IR}/L_{CO} is proportional to the star formation efficiency, defined as the rate of star formation per unit H_2 mass.

We are conducting a survey of the J = 1 → 0 $^{12}C^{16}O$ emission from a sample of galaxies of modest size in order to estimate the amount of material available to form stars. Dwarfs are the most abundant type of galaxy in the universe. They appear to be structurally simple and without the complex gas dynamics, such as spiral shocks, which can complicate the interpretation of processes in large star-forming galaxies. On the average, dwarf galaxies are closer than the giants and may therefore be studied in greater detail.

2. OBSERVATIONS

We have used the AT&T Bell Laboratories 7-m telescope and the National Radio Astronomy Observatory 12-m telescope to search for CO emission from 22 galaxies to date. Our sample is deliberately heterogeneous, reflecting the variety of small galaxies. Our selection criteria are: (1) modest angular size so that the observed CO line strength is a good measure of the total line flux; (2) detection in the IRAS Point Source Catalog, so that the total far-infrared luminosity is known; (3) far-infrared luminosities less than about $10^{10} L_{\odot}$. Our results are presented in Table 1 and Figures 1 and 2.

3. ANALYSIS

In Figure 1 we present a plot of far-infrared luminosity versus CO luminosity, along with three lines showing the L_{CO}/L_{IR} relations found by Young *et al.* to fit data for giant galaxies of different average dust temperature. These relations

Carol J. Lonsdale Persson (Editor)
Star Formation in Galaxies

TABLE 1

J = 1 → 0 CO Observations of Galaxies of Modest Size

Name	Type	Distance (Mpc)	$\int T_R^* dv \equiv S$ (K^R - km/s)	$4\pi D^2 S$ (K-km/s-Mpc^2)	V_{LSR} (km/s)	L_{FIR} ($L_\odot$)	M_{HI} ($M_\odot$)	M_{H_2} ($M_\odot$)[1]	$2.58F_{60} + F_{100}$ (Jy)[2]
CPG 330	[B] SBcII	3.1	-0.01 ± 0.15	$-0.1 \pm 1.8 \times 10^1$	359	7.2×10^7	8.8×10^7	$<3.0 \times 10^6$	12.5
Haro 2	[N] Im(p)	20.5	0.94 ± 0.22	$5.0 \pm 1.2 \times 10^3$	1435:	4.4×10^9	4.6×10^8	1.7×10^8	17
Haro 3	[N] Sm?	13.9	0.96 ± 0.28	$2.3 \pm 0.7 \times 10^3$	930:	2×10^9	5.4×10^8	7.8×10^7	17
DDO 154	[B] -	10	0.19 ± 0.10	$2.4 \pm 1.2 \times 10^2$	375	$<1.5 \times 10^8$	2.5×10^9	$<4.1 \times 10^7$	< 2.5
IC 10	[B] I	3.0	1.01 ± 0.10	$1.1 \pm 0.1 \times 10^2$	-330	1.9×10^8	--	9.4×10^6	35
Mk 86	[B] ScIIIp	7.0	0.05 ± 0.27	$0.3 \pm 1.7 \times 10^2$	449	4.2×10^8	2.4×10^8	$<3.2 \times 10^7$	14
Mk 527	[B] -	47.4	0.40 ± 0.12	$1.1 \pm 0.3 \times 10^4$	3554	2.5×10^{10}	8.4×10^8	9.4×10^8	18.5
NGC 185	[B] dE3p	0.7	0.35 ± 0.15	2.2 ± 0.9	195	9.5×10^5	4×10^5:	1.9×10^5	3.2
NGC 205	[B] SO/E5p	0.7	-0.02 ± 0.25	-0.1 ± 1.5	230	1.4×10^6	4×10^5:	$<2.5 \times 10^5$	4.8
NGC 1569	[B] SmIV	3.1	-0.24 ± 0.19	$-2.8 \pm 2.3 \times 10^1$	-83	9.8×10^8	1.7×10^8	$<1.5 \times 10^6$	170
NGC 2814	[B] -	23.2	-0.03 ± 0.17	$-0.2 \pm 1.1 \times 10^3$	1740	1.9×10^9	--	$<1.7 \times 10^8$	5.9
NGC 2976	[B] SdIII	3.1	1.2 ± 0.2	$1.5 \pm 0.2 \times 10^2$	13	3.2×10^8	--	1.3×10^7	56
NGC 3274	[B] SIV	6.4	0.1 ± 0.14	$5.0 \pm 7.2 \times 10^1$	540	1.3×10^8	7×10^8	$<1.7 \times 10^7$	5.3
NGC 3738	[B] SdIII	5.4	-0.02 ± 0.06	$-0.6 \pm 2.1 \times 10^1$	225:	1.3×10^8	3×10^8	$<3.1 \times 10^6$	7.4
NGC 4449	[N] SmIV	5.4	>2.5 ± 0.5	$>9.2 \pm 1.8 \times 10^2$	244	3.2×10^9	2×10^9	$>3.2 \times 10^7$	180
NGC 4605	[B] ScIII	4:	1.3 ± 0.3	$2.6 \pm 0.6 \times 10^2$	141	5.8×10^8	--	2.2×10^7	60
NGC 5506	[B] -	24.2	0.31 ± 0.28	$2.3 \pm 2.1 \times 10^3$	1815	1.1×10^{10}	1.2×10^9	$<5.5 \times 10^8$	31
NGC 7800	[N] Im	25.8	-0.38 ± 0.37	$-3.2 \pm 3.0 \times 10^3$	1950	2.4×10^9	3.4×10^8	$<9.5 \times 10^7$	6.0
I Zw 33	[B] Smp?	34.6	1.55 ± 0.19	$2.3 \pm 0.3 \times 10^4$	2502	6.0×10^{10}	1.7×10^9	2.0×10^9	84
I Zw 89	[B] Sb	31.1	1.96 ± 0.26	$2.4 \pm 0.3 \times 10^4$	2329	8.4×10^9	2.4×10^9	2.0×10^9	14
II Zw 40	[N] -	10.1	0.62 ± 0.29	$7.9 \pm 3.7 \times 10^2$	800	1.4×10^9	4.5×10^8	2.7×10^7	23
III Zw 102	[B] Sp	21.7	3.0 ± 0.24	$1.8 \pm 0.1 \times 10^4$	1626	1.2×10^{10}	2.3×10^9	1.5×10^9	42

Telescope: [B] Bell Telephone Laboratory 7m; [N] NRAO 12m

1. M_{H_2} was calculated from $M_{H_2}(M_\odot) = 1.07 \times 10^6 D^2(\text{Mpc}) \int T_R^* dv$ [Bell 7m] and $M_{H_2}(M_\odot) = 4.25 \times 10^5 D^2(\text{Mpc}) \int T_R^* dv$ [NRAO 12m]. Observations with the signal-to-noise ratio greater than 2 were treated as detections. Upper limits for M_{H_2} are 2σ.

2. $[2.58F_{60} + F_{100}] = L_{IR}(L_\odot)/6 \times 10^5 D^2(\text{Mpc})$ and is proportional to the integrated far-infrared flux.

extend reasonably well to include the objects of low luminosity in our sample. The center line in the figure corresponds to $L_{IR}/L_{CO} = 25$, which is about the average value for our sample.

Luminosity-luminosity plots such as Figure 1 demonstrate that both CO and infrared emission scale with the size of the galaxy: larger galaxies, on average, have more CO and infrared emission than do smaller galaxies. Although the range of far-infrared luminosities (presumably roughly proportional to mass of young stars) reported in the literature vary over almost 7 orders of magnitude, the range of star formation efficiencies is less than 2 orders of magnitude. Moreover, some of the more efficient star-forming galaxies are dwarfs. We suggest that concentration upon infrared-luminous galaxies in a study of star formation may be misplaced effort.

Such plots alone, however, cannot be used to infer a good correlation between CO and infrared emission since, in converting the observed fluxes to luminosities, both species are multiplied by a common factor: the distance (D) squared. If the range in the quantity D^2 is comparable to or greater than the range of fluxes, then even an uncorrelated set of CO and infrared fluxes will produce a correlation in a plot of luminosity! The situation is made worse by the presence of errors

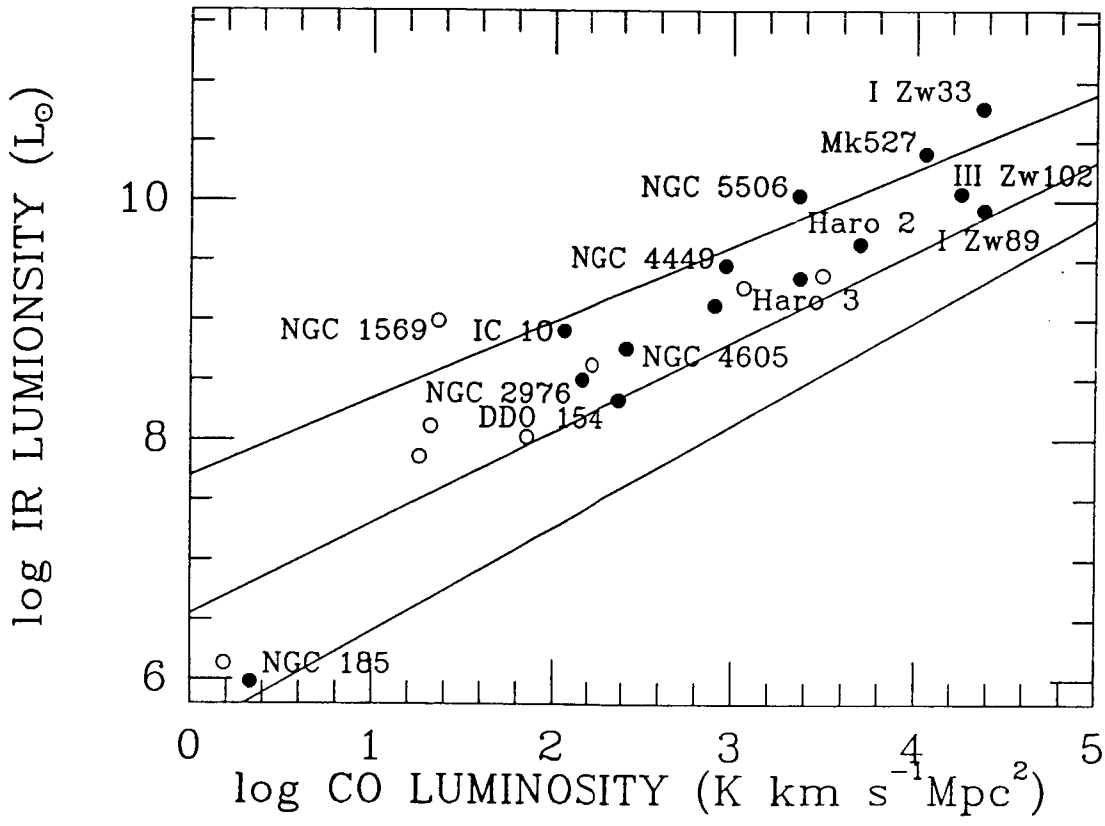

Figure 1 -- The far-infrared luminosity versus the J = 1 → 0 CO line luminosity for the sample of galaxies observed in this program. The three lines are those found by Young *et al.* for more luminous galaxies.

in the distance of the galaxies, which will tend to increase the dispersion in the common weighting factor. A distance-independent plot, such as Figure 2, is a better way to investigate the relationship between infrared and CO emission.

Figure 2 presents the CO surface brightness versus the total infrared flux, measured by $F_{IR} = 2.58S_{60}(Jy) + S_{100}(Jy)$. This plot clearly demonstrates the range of star formation efficiencies which are encountered in our sample of smaller galaxies. Objects located in the upper left of the figure are energetic star-forming galaxies: they have $L_{IR}/L_{CO} = 50$, and perhaps as high as 500! These objects include the energetic galaxies NGC 1569 and NGC 4449, as well as the mega-maser dwarf IC 10 (Henkel, Wouterloot, and Bally 1986). Although Young, Gallagher, and Hunter (1984) report a detection of NGC 1569 using the FCRAO telescope, we failed to detect it at a level 4 times fainter, indicating that the CO emission from this object comes from an area smaller than the beam of the 14-m FCRAO telescope. Objects located in the lower right of the diagram are lethargic star forming galaxies, with $L_{IR}/L_{CO} < 7$. These galaxies have a relatively large molecular content, but are not putting it to use in forming stars at a rapid rate. Objects in this category include I Zw 89 and III Zw 102.

It is interesting to note that these lethargic galaxies are relatively large spirals, whereas all of the very energetic galaxies in our sample are irregulars. Extensive spiral structure is obviously not necessary for a high efficiency of star formation.

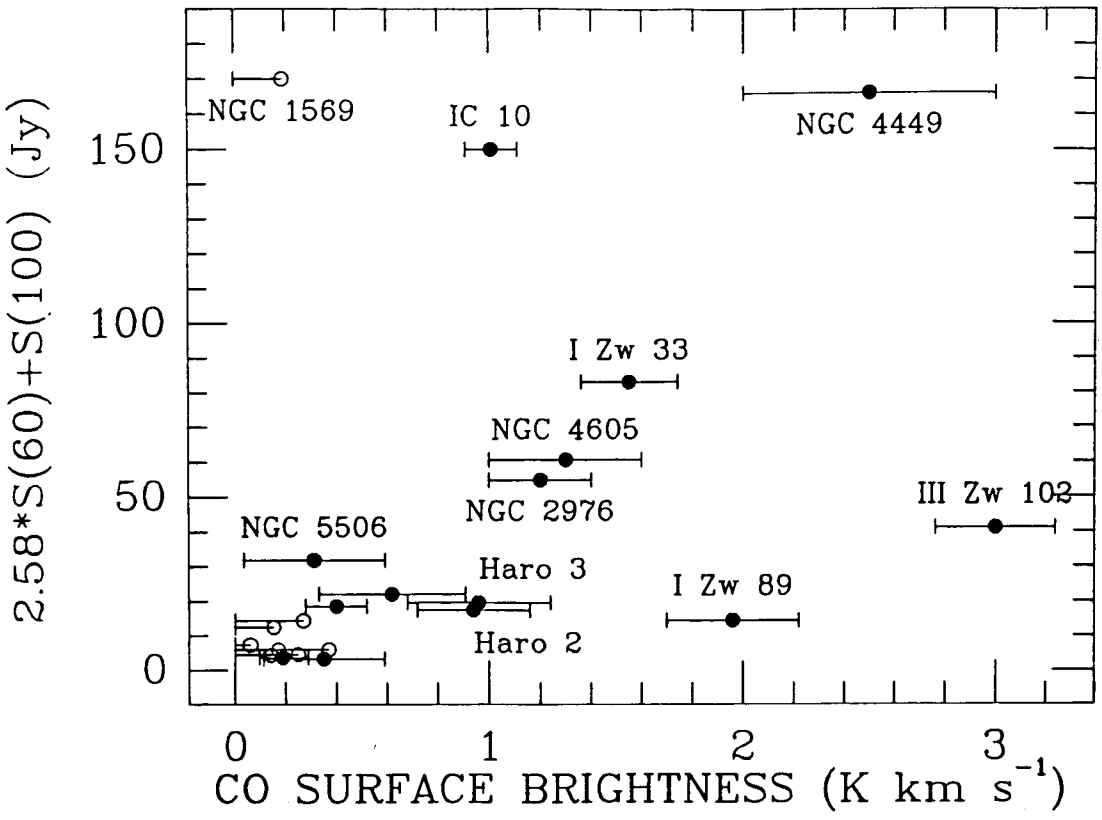

Figure 2 -- The far-infrared flux versus the J = 1 → 0 CO line flux. Upper limits are open circles. Note the wide variation in F_{IR}/F_{CO}.

A possible explanation for the high star-forming activity in irregular systems may be a higher efficiency of induced star formation (or, more significantly, molecular cloud formation) in a system having a thick gas layer. Within a thin disk, with a small scale-height gas layer, much of the pressure generated by massive star formation might be released above and below the plane of the gas layer. Only an annular region within the plane is compressed. Within an irregular galaxy or a thick disk, this pressure is confined and may therefore produce compression in all directions.

H. Thronson was partially supported by NASA grant NAG 2-134.

REFERENCES

Henkel, C., Wouterloot, J. G. A., and Bally, J. 1986, *Astr. Ap.*, 155, 193.

Rickard, L. J, and Harvey, P. M. 1984, *Astron. J.*, 89, 1520.

Telesco, C. M., and Harper, D. A. 1980, *Ap. J.*, 235, 392.

Young, J. S., Gallagher, J. S., and Hunter, D. A. 1984, *Ap. J.*, 276, 476.

Young, J. S. *et al.* 1986, *Ap. J.*, 304, 443.